AIAA 80-1117R

Experimental Investigation of Pressure Oscillations in a Side Dump Ramjet Combustor

W.H. Clark*
Naval Weapons Center, China Lake, Calif.

A two-inlet, side dump ramjet combustor configuration was tested in a connected-pipe setup using uncooled and uninsulated chamber walls. High amplitude combustion induced pressure oscillations were observed during most test conditions with a predominant frequency of around 300 Hz. Special efforts were made to relate the oscillations to longitudinal acoustic modes. A simplified no flow, uniform temperature acoustic cavity prediction method (NASTRAN) was utilized to model the longitudinal acoustic modes. This model was verified via room temperature laboratory tests using the actual test hardware and a loudspeaker as an input forcing function to excite the acoustic modes. During combustion tests, the measured oscillation modes were tentatively identified as second or third longitudinal modes or a "bulk" mode, depending on the test conditions.

Nomenclature

A	= cross-sectional area
c	= local sound speed
C_D	= fuel injector discharge coefficient
f	= frequency
L_C	= combustor length (Fig. 1)
L_I	= inlet length (Fig. 1)
M	= Mach number
p	= local static pressure
p_r	= reference sound pressure level ($=2.90\times10^{-9}$ psi)
P_T	= total pressure
T_T	= total temperature
$\dot{W}_a$	= vitiated air flow rate (lbm/s)
ΔP_I	= fuel injector pressure drop
$(\Delta p)_{\text{rms}}$	= root-mean-square pressure fluctuation at the dominant frequency
ϕ	= equivalence ratio

Subscripts

0, 1.5, 4,5	= axial stations (Fig. 1)
i	= ith longitudinal acoustic mode
$1/4$	= localized inlet 1/4-wave mode

Superscripts

$\bar{()}$	= average quantity
0	= frequency at $\bar{M}=0$

I. Introduction

A NUMBER of future tactical missile concepts employ the integral-rocket-ramjet (IRR) engine in order to provide increased range and velocity beyond that available from conventional rocket motors. Most of the liquid fueled ramjet engines under development use a sudden-expansion type of combustor, in which flameholding is achieved primarily in the recirculation zone located at the expansion or "dump" station. Several current ramjet engines have exhibited excessively high amplitude, combustion-induced pressure oscillations during ground testing in connected-pipe, and freejet testing modes.[1,2] (A description of these modes of ramjet engine testing has been provided elsewhere.[3]) Pressure oscillations with frequencies ranging from tens to several thousands of Hertz have been observed. From a practical standpoint, the most troublesome oscillations are at frequencies ranging from approximately 100–500 Hz. In this frequency range, root-mean-square (rms) pressure oscillation amplitudes up to 20% of the mean combustion chamber static pressure are not uncommon. At present, the primary concern is the effect that these low frequency (100-500 Hz) oscillations can have on inlet performance. A detailed discussion of the undesirable interactions between the inlet and the combustion-induced pressure oscillations has been provided in another paper.[2]

Because of the serious design problems associated with these oscillations, the ramjet industry has recently taken a renewed interest in the old problem of combustion instabilities. Efforts are underway to acquire and categorize data which describe the oscillatory behavior of a range of different modern ramjet engine concepts. The experiments to be described in this paper are one part of these overall efforts.

II. Test Configurations

In several IRR engines, the inlet air is routed to the combustor via two or four ducts and dumped into the combustor through ports in the sides of the chamber. A two-inlet, "side dump" configuration, which was known to exhibit high-level pressure oscillations, was selected for this investigation. The baseline configurations to be discussed herein is illustrated in Fig. 1. Heated air, which simulates the appropriate flight Mach number and altitude conditions, exited a plenum chamber and entered the engine through two choked converging-diverging nozzles. For reasons that will be discussed shortly, it is important in connected-pipe tests to simulate the supercritical operation of an actual inlet. Hence, the converging-diverging nozzles provided a choked throat followed by a normal shock system standing in the diverging section of each inlet nozzle.

Fuel was introduced through the contra-steam fuel injectors located as shown in Fig. 1. Details of the simple fixed-orifice fuel injectors are shown in Fig. 2. The fuel-air mixture was then dumped into the combustion chamber through the side ports, as illustrated in Fig. 1. The mixture was initially ignited via the H_2-O_2 igniter torch shown in Fig. 1, and flameholding was achieved in the recirculating flow between the dump and dome stations. The exhaust gases exited the combustor through the fixed nozzle with the area ratio indicated in Fig. 1.

Presented as Paper 80-1117 at the AIAA/SAE/ASME 16th Joint Propulsion Conference, Hartford, Conn., June 30-July 2, 1980; submitted Aug. 25, 1980; revision received June 16, 1981. This paper is declared a work of the U.S. Government and therefore is in the public domain.

*Aerospace Engineer, Code 3246. Member AIAA.

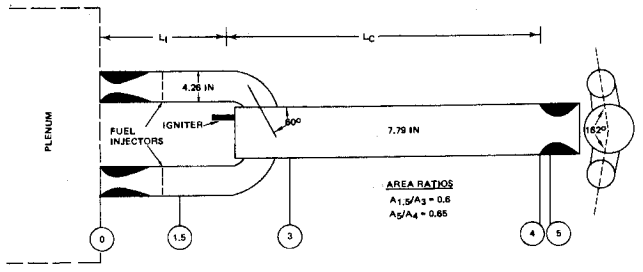

Fig. 1 Side dump ramjet engine test configuration.

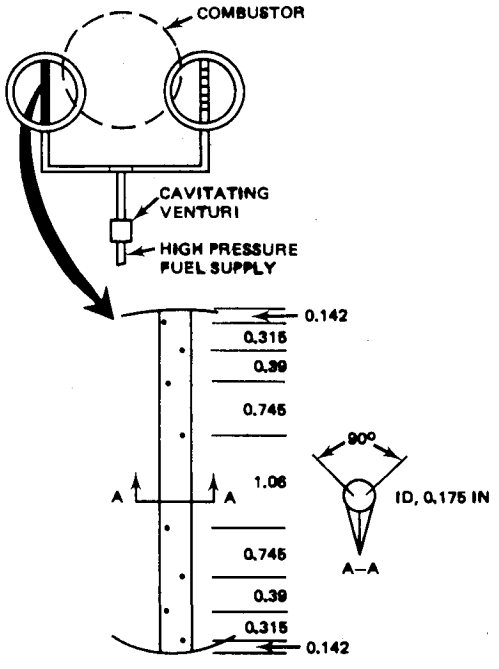

Fig. 2 Fixed orifice contra-stream fuel injectors (eight holes of 0.04-in. diam, $C_D = 0.56$).

Two modifications to this baseline configuration were also tested. All three configurations to be discussed are shown in Fig. 3. Configuration I is the baseline described above. In configuration II, the inlet ducting length (L_I) was increased; in configuration III, the combustion chamber length (L_C) was decreased. The relevant dimensions for each configuration are shown in Fig. 3. The three configurations differed only in the length dimensions (L_I and L_C) as shown.

III. Test Procedures

As previously mentioned, all testing was accomplished in a connected-pipe mode. The facility air was heated in a propane burner, and oxygen was then added to restore the proper oxygen mass fraction in the air. The desired vitiated air flow rate and temperature, as measured in the plenum, were held constant during each run. The ramjet fuel flow rate was then set to give a desired equivalence ratio (ϕ) and the mixture was ignited. The combustion chamber walls were uncooled, uninsulated, thin (0.10 in.) stainless steel. Under these conditions, the actual hot firings were of short duration (typically 2-4 s) in order to avoid damaging the test hardware.

Since the primary purpose of these tests was to characterize the modes of oscillation, the inlets and combustor were well instrumented with high-frequency piezoelectric pressure transducers. These high-frequency pressure transducers were distributed axially, as shown in Fig. 4, in order to identify longitudinal modes. The transducers used were a mixture of Kistler Models 216M11 and 616A fitted inside water-cooled adaptors which were directly mounted onto the test item such

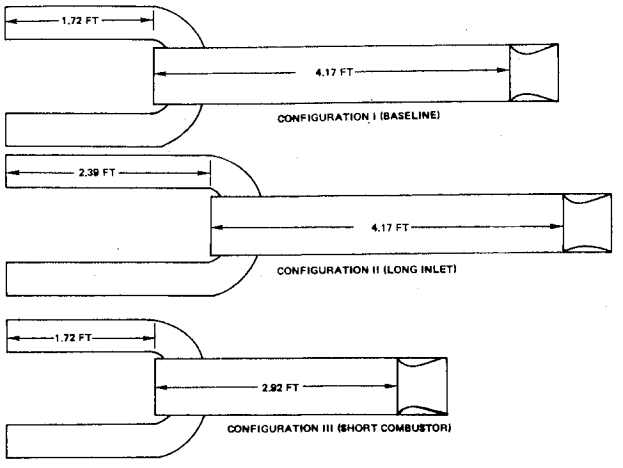

Fig. 3 Ramjet engine configurations tested.

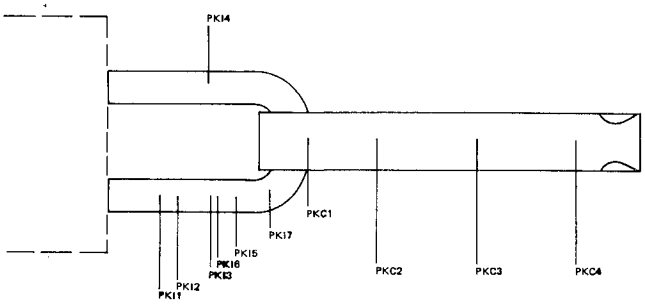

Fig. 4 High-frequency pressure transducer locations.

that the transducers' sensitive face was flush with the inside walls of the inlets and combustor. The transducer outputs were recorded on oscillographs and analog tapes for further analysis. The high-frequency analog data were later analyzed using a Hewlett-Packard 5420A digital signal analyzer to generate power spectral density plots and to compute the relative phases between transducer signals at the frequency components of interest. Steady-state data from strain gage pressure transducers, thermocouples, and flowmeters were recorded on digital tapes for later processing.

The combustion chamber total temperature (T_{T_4}) and total pressure (P_{T_4}) at station 4 were estimated based on the measured static pressure at station 4, the measured mass flow rate, and the known area ratio (A_4/A_5). Similarly, the inlet Mach number ($M_{1.5}$) and total pressure ($P_{T_{1.5}}$) were estimated from the measured static pressure, total temperature, mass flow, and known inlet area. Tests were conducted with air flow rates ranging from $6 \leq \dot{W}^a \leq 20$ lb/s, inlet total temperatures from $440 \leq T_{T_0} \leq 940$°F, and equivalence ratios from $0.4 \leq \phi \leq 1.2$. Some typical results for each configuration were selected for discussion in this report. The pertinent inlet air and fuel flow conditions and the corresponding computed engine conditions are given in Tables 1 and 2, respectively. RJ-4 fuel was used in all the tests discussed here. The combustion-induced pressure oscillations observed during each test condition of Tables 1 and 2 will be presented in Sec. V.

IV. Acoustic Cavity Tests

Traditionally, combustion instabilities in liquid and solid propellant rocket motors have been related to the natural acoustic modes that could exist in a particular chamber. If a mechanism exists for unsteady heat release and if the phase and spatial location of this unsteady heat release maintains certain relationships with respect to the natural acoustic oscillations, then it is possible for small acoustic pressure

fluctuations to grow in amplitude. Unstable growth of the pressure oscillations will generally occur if the unsteady heat release occurs in-phase with the acoustic pressure oscillations and at a spatial location that does not lie on a pressure node. The class of ramjet combustors under consideration here certainly possess potential mechanisms for unsteady heat release. It is reasonable to assume that the fuel flow rate remains constant despite the pressure oscillations, as evidenced by the large fuel injector pressure drops shown in Table 2. Hence, if the inlet air flow rate fluctuates, then the fuel-to-air ratio of the mixture entering the combustor will also fluctuate. The phasing and spatial location of the unsteady heat release will be a complicated function of time lag associated with chemical kinetics, droplet burning, spray combustion, and turbulent mixing processes. These time lag mechanisms are, of course, functions of chamber pressure and temperature, method of fuel injection, and the geometric configuration of the dump station.

These side dump combustors also possess another potential mechanism for sustaining unsteady heat release that may not be related to the acoustic modes. This is a fluid mechanical phenomenon associated with the natural unsteady flow at the dump station. Regular vortex shedding at the dump could provide a means for unsteady heat release. These fluid mechanical phenomena are likely to be quite complicated, and an adequate characterization of them would require far more experimental effort than has been expended in the present tests. An adequate first-order characterization of the natural acoustic modes of the ramjet engines under consideration is, however, relatively straightforward.

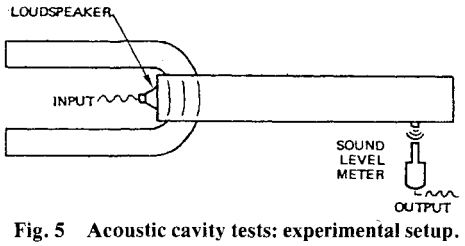

Fig. 5 Acoustic cavity tests: experimental setup.

Table 1 Test conditions

Configuration	Flow condition	$\dot{W}_a$, lbm/s	T_{T_0}, °F	ϕ[a]
I (baseline)	1	20	640	0.45
	2	20	635	0.63
	3	20	640	0.75
	4	20	638	1.05
II (long inlet)	5	20	643	1.15
	6	13.8	670	0.6
	7	13.1	650	0.9
III (short combustor)	8	21	661	0.77
	9	21	657	0.59

[a] RJ-4 fuel was used, with a stoichiometric fuel/air ratio of 0.07.

As mentioned earlier, the pressure oscillations of primary concern have frequencies ranging from approximately 100–500 Hz. This implies that, if natural acoustic oscillations are involved, the longitudinal modes are of interest. A proper analytical tool for the prediction of these longitudinal acoustic modes would have to include several factors that are not generally available in most prediction codes. These factors are: 1) the finite acoustic admittance of the normal shock in the inlet diffuser and the choked exit nozzle (these determine the respective upstream and downstream boundary conditions for the longitudinal acoustic waves); 2) the variable temperature (or sound speed) throughout the inlet and combustor; and 3) the relatively large mean subsonic Mach number in the inlets and combustor. While these factors are not conceptually difficult to include in a prediction method, such a code was not readily available to the author. A prediction code was available, however, which accounts for factor 2, above. This prediction code is the acoustic cavity option of the well-known NASTRAN computer program.[4]

The NASTRAN code was used to predict the natural, undamped longitudinal acoustic modes of the three inlet/combustor configurations described earlier. The engine walls were assumed to be rigid, while the upstream normal shock and downstream choked exit nozzle were treated as ideal acoustically closed boundaries. The temperatures in the inlets and combustor were based on the experimental values given in Table 2. The temperature was assumed to change abruptly at the dump from the inlet temperature to a uniform chamber temperature. The acoustic cavity option of the NASTRAN code was originally designed to handle solid rocket motors, which typically consist of an axisymmetric central cavity and a number of symmetrically placed slots which are cut into the propellant. The methods by which the solutions for the pressures in the slots and the central cavity are coupled have been described.[4] For the present application, the two inlets of the ramjet engine were treated as "slots," while the combustor corresponded to the axisymmetric central cavity.

Before the results obtained during the hot firings are discussed, the NASTRAN predictions will be compared with experimental results obtained under more ideal laboratory conditions. The actual baseline hardware (configuration I) was tested for longitudinal acoustic modes under room temperature conditions with the inlet and exit areas sealed shut. The inlet/combustor cavities were acoustically excited by means of a loudspeaker located at the dome section, as indicated in Fig. 5. The voltage at the speaker was servo controlled to maintain a constant amplitude voltage over the frequency range of interest. The system response was measured with a Bruel & Kjoer precision sound level meter (Type 2209) which was placed at the various pressure transducer ports along the inlet/combustor walls. The speaker response, as measured with the sound level meter, is shown in Fig. 6. Typical output amplitude response functions at two different axial locations are shown in Fig. 7. In Figs. 6 and 7, the output sound pressure level is given in decibels and is

Table 2 Estimated parameters for conditions of Table 1

Configuration	Flow condition	T_{T_4}, °F	P_{T_4}, psia	$P_{T_{1.5}}$, psia	$M_{1.5}$	M_4	$\Delta P_1/P_{T_4}$
I	1	1845	65.7	77.6	0.38	0.43	1.6
	2	2382	76.2	88.5	0.34	0.43	2.2
	3	3036	83.0	95.1	0.30	0.43	3.8
	4	3110	87.4	99.8	0.29	0.43	5.9
	5	3287	88.6	101.7	0.28	0.43	6.9
II	6	2400	48.5	56.2	0.35	0.43	1.7
	7	2588	54.6	63.5	0.3	0.43	4.5
III	8	3191	83.2	94.1	0.3	0.43	4.2
	9	No sustained ignition					

defined in the usual manner as

$$\text{SPL} = 20 \log (p/p_r) \quad (1)$$

From the well-defined resonant modes, such as those displayed in Fig. 7, the modal amplitude and frequency can be determined. The amplitude distribution for the first three longitudinal modes is shown in Fig. 8. Also shown in Fig. 8 is the amplitude distribution for the undamped modes as predicted by the NASTRAN model. From this figure, it is clear that the predicted and measured frequencies are in excellent agreement, while the relative pressure amplitude axial distributions are in reasonable agreement except in the inlet stations.

Referring again to Fig. 7, it can be seen that a localized resonant mode appears in the inlet but is completely absent in the combustor. This mode, which was not predicted by the NASTRAN model, occurs with a frequency of approximately 145 Hz. The location and frequency of this mode suggest the presence of an inlet 1/4-wave "organ pipe" mode. The "effective" acoustic length of the inlet for a 1/4-wave mode is

$$L = c/4f^{\,0}_{1/4} = 1.9 \text{ ft} \quad (2)$$

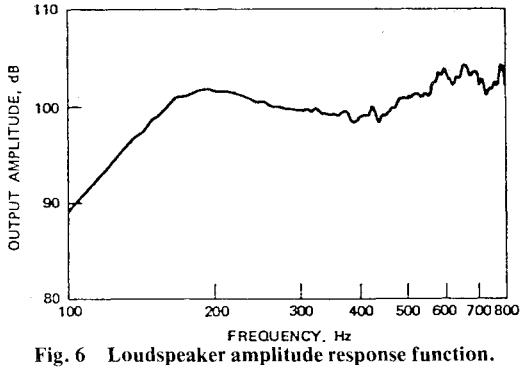

Fig. 6 Loudspeaker amplitude response function.

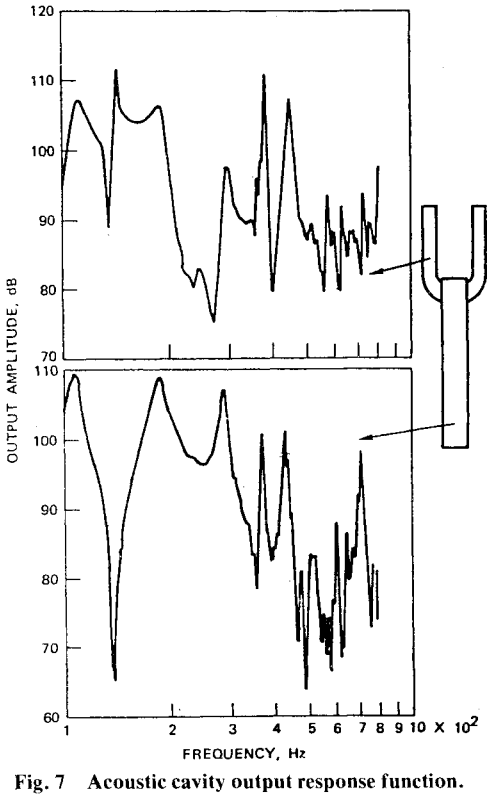

Fig. 7 Acoustic cavity output response function.

for $c = 100$ ft/s and $f^{\,0}_{1/4} = 145$ Hz. A comparison between the theoretical amplitude distribution and the measured pressures is shown in Fig. 9. While the quantitative agreement in poor, the qualitative trend of the data supports the argument that a localized inlet 1/4 wave does exist. This mode appears to play an important role when combustion instabilities are present, as will be discussed below.

V. Combustion Tests

A selected number of tests for each of the three configurations was summarized in Tables 1 and 2. The oscillations measured during the tests were typical of those observed during the entire test series, which consisted of approximately 150 hot firings. Typical oscillograph traces of the pressure oscillations recorded during testing of configuration I at flow condition 2 (Tables 1 and 2) are shown in Fig. 10. The relative pressure amplitudes, as measured by the high-frequency transducers during this test, are plotted vs axial location in Fig. 11. The relative pressure amplitudes are plotted to facilitate comparisons with the predicted natural modes. The plotted experimental data points can be converted to a more physically meaningful parameter $[(\Delta p)_{\text{rms}}/P_{T_4}]$ by multiplying the plotted value by the conversion factor given in the figure caption. In Fig. 11, the experimental values are compared with the mode shape for the *second* longitudinal mode predicted by the NASTRAN model. Also in Fig. 11, the phases of the oscillations at the fundamental frequency (280 Hz) at each station are plotted relative to the phase of the most upstream pressure transducer (PKI1, Fig. 4). The pressure amplitude distributions are in reasonable agreement with the predicted second longitudinal mode shape, except in the inlet ducting, which was also the case during the room temperature acoustic cavity tests. The relative phases further support the contention that the second longitudinal mode has been excited. The oscillations at transducer stations PKI7, PKC1, and PKC2 are essentially ± 180 deg out-of-phase with PKI1, whereas the oscillations at PKC3 and PKC4 are in-phase with PKI1. A 180-deg phase shift would be expected to occur across each pressure node for the ideal acoustic cavity resonant modes.

The fundamental oscillation frequency for configuration I varied with equivalence ratio as shown in Fig. 12. Also indicated in this figure are several predicted frequencies based on the experimental inlet/combustor temperatures from

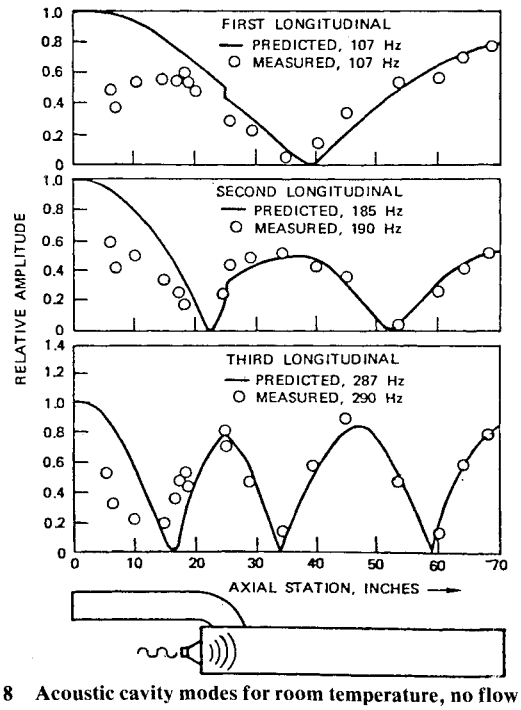

Fig. 8 Acoustic cavity modes for room temperature, no flow tests.

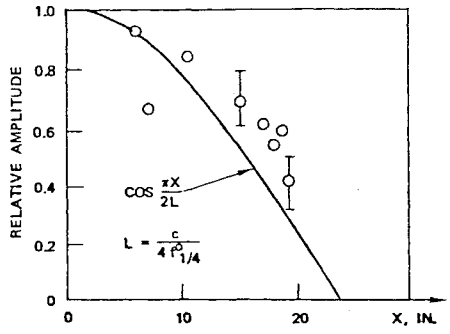

Fig. 9 Comparison of experimental pressure amplitude and theoretical inlet 1/4-wave mode shape ($c = 1100$ ft/s, $f^0_{1/4} = 145$ Hz).

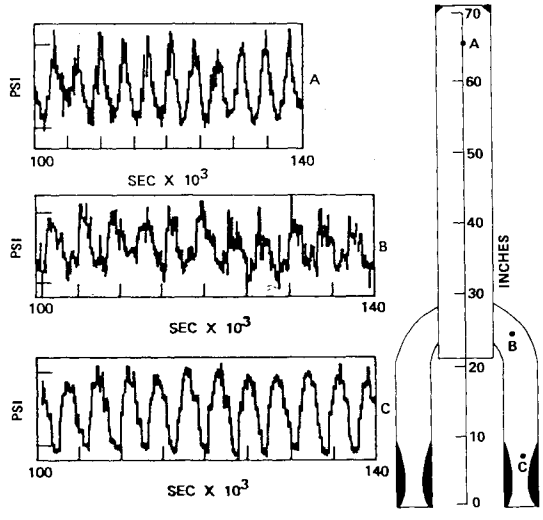

Fig. 10 Typical waveforms for configuration I, flow condition 2.

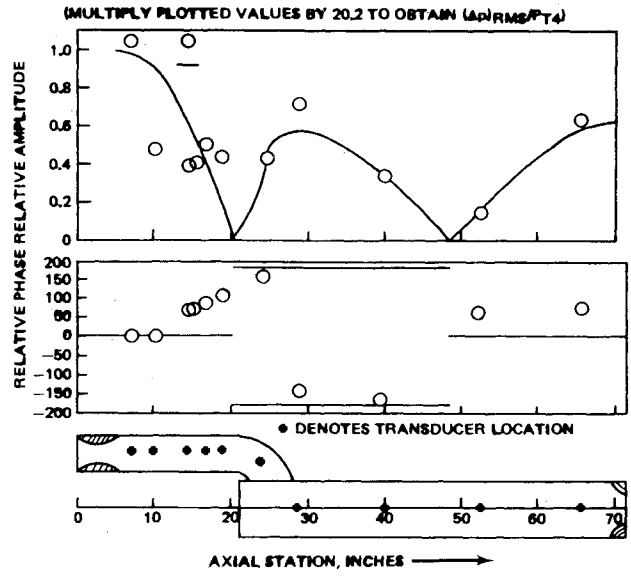

Fig. 11 Relative amplitude and phase distributions for configuration I, flow condition 2.

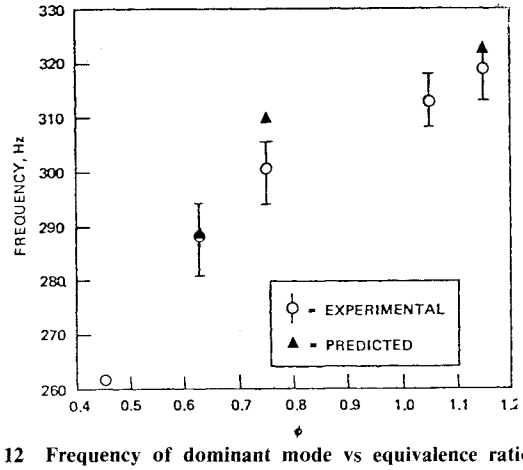

Fig. 12 Frequency of dominant mode vs equivalence ratio, configuration I, flow conditions 1–5.

Table 2. The predicted frequencies, as shown in Fig. 12, were computed by the NASTRAN program and corrected for the effects of the nonzero subsonic Mach number in the inlet/combustor cavities. It can be shown that the frequencies (f_i) of longitudinal acoustic modes in a duct with a subsonic mean Mach number (M) are related to the frequencies for zero Mach number by[1]

$$f_i = (1 - \bar{M}^2) f_i^0 \tag{3}$$

In the ramjet engine, the Mach number is not uniform throughout the inlet/combustor chambers and varies with equivalence ratio. In order to roughly account for these variations, a Mach number was computed by simply averaging the Mach numbers at stations 1.5 and 4 for flow conditions 2, 3, and 5 of Tables 1 and 2; i.e.,

$$\bar{M} = \tfrac{1}{2}(M_{1.5} + M_4) \tag{4}$$

The computed undamped natural frequencies (f_2^0) for these three conditions were then corrected via Eqs. (3) and (4). The values are indicated in Fig. 12 and Table 3. It is gratifying to note that both the trends and magnitudes (to within 5%) are correctly predicted.

The oscillatory characteristics of configuration II are summarized in Figs. 13 and 14. Under most conditions, this configuration exhibited a dominant frequency of around 300 Hz. The modal shape at this frequency, as measured under flow condition 7 (Table 1), is shown in Fig. 13. In this case the measured amplitude and phase distributions are compared with the *third* longitudinal mode. Although the amplitude and phases of this mode resemble the predicted third longitudinal mode, the frequency (Table 3) actually lies between the values predicted for the second and third modes. A completely different mode was observed at the low equivalence ratio fuel flows at flow condition 6. This mode, at a measured frequency of 138 Hz, is compared with the predicted first longitudinal mode in Fig. 14. In this case, the data do *not* clearly indicate that the predicted acoustic mode was excited. Indeed, the data for flow condition 6 resemble the results reported by Rogers[2] for a ramjet engine that is very similar to the engine configurations under consideration here. Rogers' results suggested the presence of a bulk mode of oscillation in which the combustor and inlets oscillate in-phase at a frequency approximately equal to an inlet 1/4 wave. It is straightforward to calculate the frequency for an inlet 1/4 wave based on the results obtained during the acoustic cavity tests. From Eq. (2), it was shown that the effective inlet length for configuration I is $L = 1.9$ ft. The inlets of configuration II are 8 in. longer than those of configuration I. Hence,

$$f^0_{1/4} = \frac{c}{4L} = \frac{1580}{(4)\ (2.57)} = 154 \text{ Hz}$$

In this case, the mean Mach number (M) to be used in Eq. (3) is $M_{1.5}$. Hence,

$$f_{1/4} = (1 - 0.35^2)\,154 = 135 \text{ Hz}$$

Table 3 Experimental and predicted frequencies

Configuration	Test condition	Experimental frequency, Hz	$(\Delta p)_{rms}/P_{T_4}$, %	Predicted frequencies, Hz f_1	f_2	f_3	$f_{1/4}$
I	1	262	8	...	...	...	178
	2	288	21	185	288	511	184
	3	300	20	194	315	549	189
	4	312	19	...	...	...	191
	5	319	13	198	323	566	192
II	6	138	16	148	269	434	135
	7	330	14	150	277	439	140
III	8	313(400)	3	195	416	553	189
	9	175	...	...	...	...	...

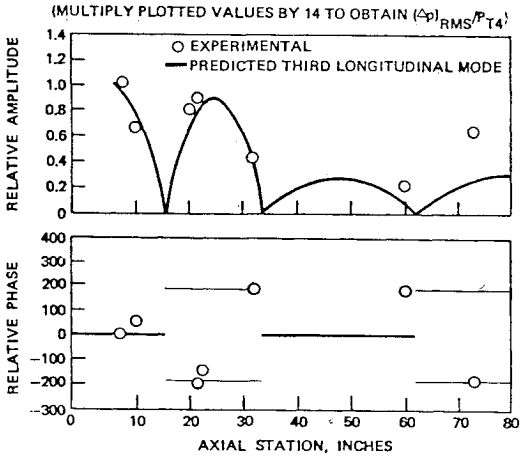

Fig. 13 Relative amplitude and phase distributions for configuration II, flow condition 7.

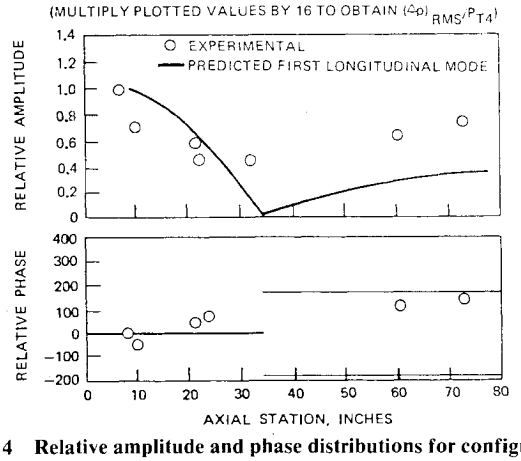

Fig. 14 Relative amplitude and phase distributions for configuration II, flow condition 6.

Finally, for configuration III the oscillation frequencies tended to be in the range of 300–400 Hz under most conditions. During this test series, only pressure transducers PKI1 and PKC4 were available; hence, an amplitude distribution was not obtained. A power spectral density plot for station PKI1 under flow condition 8 is shown in Fig. 15. Two modes are present—at approximately 300 and 400 Hz. Under the lean fuel setting of flow condition 9, a low frequency mode at 175 Hz was observed. Although ignition was not sustained for this condition, it is likely that this was the same bulk mode observed for flow condition 6.

VI. Summary

Through a combination of theoretical (NASTRAN) predictions and room temperature laboratory tests, the natural acoustic modes of the baseline inlet/combustor cavities without flow were well defined. A localized, 1/4-wave acoustic mode of the inlet was experimentally detected.

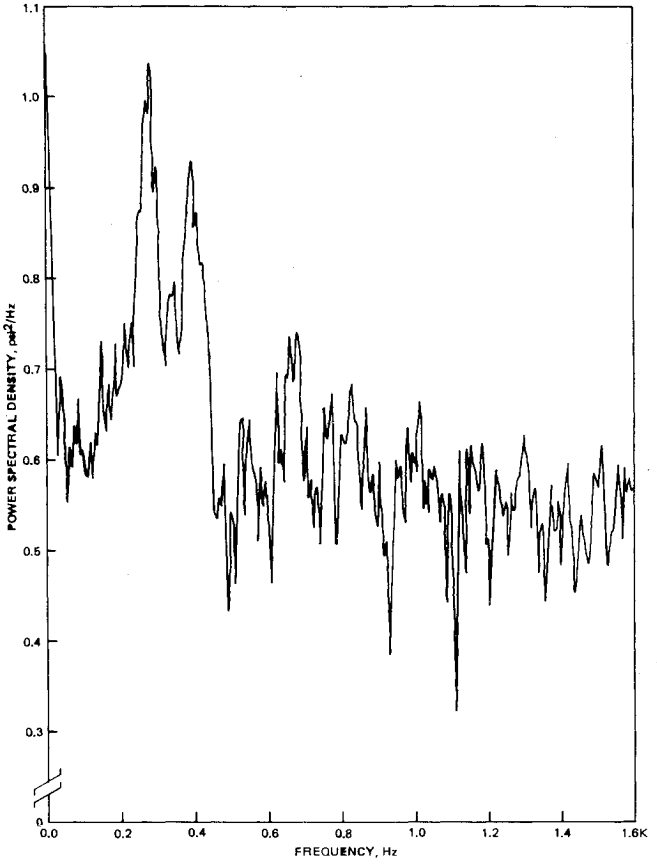

Fig. 15 Power spectral density from transducer PKI1, configuration III, flow condition 8.

During actual combustion tests, pressure oscillations occurred at a frequency of approximately 300 Hz for all three configurations and over most flow conditions. For configuration I, this 300-Hz mode was identified as the second longitudinal acoustic mode by comparison with the theoretical mode shape and with theoretical predictions of the frequencies. For configuration II, the dominant 300-Hz mode shape and phase distribution suggested that the third longitudinal mode was excited, although the predicted and measured frequencies were not in agreement. For configuration III, the data indicated that two modes at roughly 300 and 400 Hz were present, which suggested that the second and third longitudinal acoustic modes were present. Again, the measured and predicted frequencies were not in agreement. This lack of quantitative agreement is not surprising in view of the simplifications of the acoustic model. The reader is reminded that the NASTRAN model ignores the

effects of the mean flowfield and does not include realistic upstream and downstream boundary conditions.

Under lean fuel flow conditions, another low-frequency mode was observed. The frequency of this mode was shown to be very close to a localized, 1/4-wave mode of the inlet, and the mode shape and phase distribution suggested that the bulk mode discussed by Rogers was present.

All three of the configurations studied used the same dump station geometry. Since the dominant oscillation frequency for all three configurations was approximately the same (300 Hz), it is speculated that a mechanism for unsteady heat release is associated with the fluid dynamics of the dump station. In the case of Configuration I, the second longitudinal acoustic mode coincidentally happened to be at around 300 Hz. This is probably why this mode could be clearly identified for configuration I but not for the other two configurations. The data presented here and by Rogers also reveal that modern ramjet engines of identical or very similar configurations can exhibit different modes of oscillation depending on inlet air flows, upstream acoustic boundary conditions, or methods of fuel injection.

References

[1] Rogers, T., "Ramjet Inlet/Combustor Pulsations Study," Naval Weapons Center, China Lake, Calif. NWC TP 6053, Jan. 1980.

[2] Rogers, T., "Ramjet Inlet/Combustor Pulsations Analysis and Test," Naval Weapons Center, China Lake, Calif., NWC TP 6155, Feb. 1980.

[3] Dunsworth, L.C. and Reed, G.J., "Ramjet Engine Testing and Simulation Techniques," *Journal of Spacecraft and Rockets*, Vol. 16, Nov.-Dec. 1979.

[4] Herting, D.N., Joseph, J.A., Kuusinen, L.R., and MacNeal, R.H., "Acoustic Analysis of Solid Rocket Motor Cavities by a Finite Element Method," Air Force Rocket Propulsion Laboratory, AFRPL-TR-71-96, 1971.